

# Temperature and performance evaluation of multiprocessors chips by optimal control method

Porya Soltani Hanafi Por<sup>1</sup>, Abbas Ramazani<sup>1</sup>, Mojtaba Hosseini Toodeshki<sup>2</sup>

<sup>1</sup>Department of Electrical Engineering, Bu-Ali Sina University, Hamedan, Iran

<sup>2</sup>Electrical Engineering Group, Branch of Control, Hamedan University of Technology, Hamedan, Iran

## Article Info

### Article history:

Received Jun 20, 2022

Revised Jul 14, 2022

Accepted Sep 30, 2022

### Keywords:

Asymmetric multi-core  
processor  
ODROID-XU4  
Optimal control  
Performance  
Temperature

## ABSTRACT

Multi-core processors support all modern electronic devices nowadays. However, temperature and performance management are one of the most critical issues in the design of today's microprocessors. In this paper, we propose a framework by using an optimal control method based on fan speed and frequency control of the multi-core processor. The goal is to optimize performance and at the same time avoid violating an expected temperature. Our proposed method uses a high-precision thermal and power model for multi-core processors. This method is validated on asymmetric ODROID-XU4 multi-core processor. The experimental results show the ability of the proposed method to achieve the adequate trade-off between performance and temperature control.

*This is an open access article under the [CC BY-SA](#) license.*



## Corresponding Author:

Abbas Ramazani  
Department of Electrical Engineering, Bu-Ali Sina University  
Hamedan, Iran  
Email: a.ramazani@basu.ac.ir

## 1. INTRODUCTION

Nowadays the problem of temperature management of multi-core processors has become a critical problem for developers due to the increase in computing power and integration density. The power consumption generates heat that increase the chips temperature. High temperature decreases the reliability and life of the chips. Therefore, providing a solution for proper temperature and performance management in the multi-core processor is inevitable [1], [2].

To control the temperature of chips, embedded systems usually use dynamic thermal management (DTM) techniques. These techniques usually try to adjust the processor voltage and frequency to control power consumption and temperature [3]–[5]. Many thermal management techniques have been proposed for modern chips due to increased power densities and reliability implications. When the junction or skin temperature outpaces a safe value point, the cores need to reduce the temperature by lowering the power consumption. Therefore, the lack of a dynamic thermal-power management (DTPM) algorithm can lead to reduced performance [6], [7]. For this reason, a trade-off is made between maintaining performance and controlling the temperature [8].

Thermal management techniques can be divided into two categories: the physical techniques and the techniques based on control theory. The initial simple physical technique solution to deal with temperature rises in multi-core processors was to add a heatsink to further disperse the heat generated in the processor. Sahoo *et al.* [9] reported different arrangements of heat sinks and their construction elements. Choi *et al.* [10] investigated the performance of active central processing unit (CPU) cooling heatsink with heat pipes. Siricharoenpanich *et al.* [11] studied the impact of the inclination angles of the heat pipes of CPU. Research

by Yousefi *et al.* [12] an experimental study of heat transfer performance of a CPU cooling heat pipe and examining the effects of inclination angle and nanofluids has been presented. Subsequent technologies included the addition of water cooling and liquid cooling. Nazari *et al.* [13] compared the cooling performance of the common base fluids. One of the most basic forms of DTM is known as “stop-go” [6]. Although it’s very effective in controlling the temperature but it reduces efficiency dramatically. In the second category, the control methods extracted from control theory such as proportional–integral–derivative (PID) controller [14], model predictive control (MPC) [15], stochastic control [16], nonlinear control [17], fuzzy control [18]–[20] are used to control the chip temperature. According to [21]–[23], frequency and fan speed controllers have been designed but control goals including temperature and performance control have not been examined simultaneously. According to Fu *et al.* [24] achieved control goals but the proposed thermal model is very difficult to extract and the parameters required to extract the thermal model cannot be achieved in the most of processors.

In the most of the mentioned control techniques, the core frequency and the fan speed in the design of controllers were not considered simultaneously or there is a lack in tradeoff between performance and temperature control. Therefore, in our proposed solution to solve the mentioned problems, we consider the core frequency and the fan speed as the control variables in order to make a good compromise between performance and temperature control. We used the optimal control method. The reason for selection is that the control variables have constraints and through this method we can define a tradeoff between temperature and performance by considering the constraints.

The rest of this paper is organized as follows: an overview of the proposed DTPM technique is provided in section 2. Mathematical statements are described in section 3. Experimental evaluation on the Exynos 5422 processor employed in the ODROID-XU4 board is presented in section 4. Finally, the conclusions are discussed in section 5.

## 2. PROPOSED FRAMEWORK

Effective management of performance and temperature in multi-processor systems depends critically on accurate analytical models that can be evaluated at run-time [25]. We have used the ODROID-XU4 board with Exynos 5422 processor, which has 4 cores belonging to a big cluster and 4 cores belonging to a little cluster. In this board, the frequency of large and small cores, the temperature of large cores, the CPU utilization of large and small cores and the fan speed can be accessed and observed. The temperature sensors are located only on the cores of the big cluster and temperature samples are the average temperature of cores (the accuracy of the temperature sensor of each core is 1 °C). Also, it should be noted that since this board is an asymmetric multi-core processor, by changing the frequency of one core in each cluster, the frequency of all cores in that cluster changes.

It is not possible to directly measure power in ODROID-XU4; therefore, we can calculate the power consumption of the cores indirectly. In the others word, we try to have an appropriate estimation of power consumption. The main heat generating elements in the ODROID-XU4 are A7 and A15 clusters (little and big clusters). The focus of our work is on these two clusters and thermal model for them.

We have used the framework in Figure 1. At first, the measurable data of the A7 and A15 cores including the working frequency of the cores, the temperature of the cores, and the estimation of the computing power in the execution of the benchmark programs are collected. These data are used in providing power and thermal models. In the next step, we use this model to obtain the state space and optimal controller design.

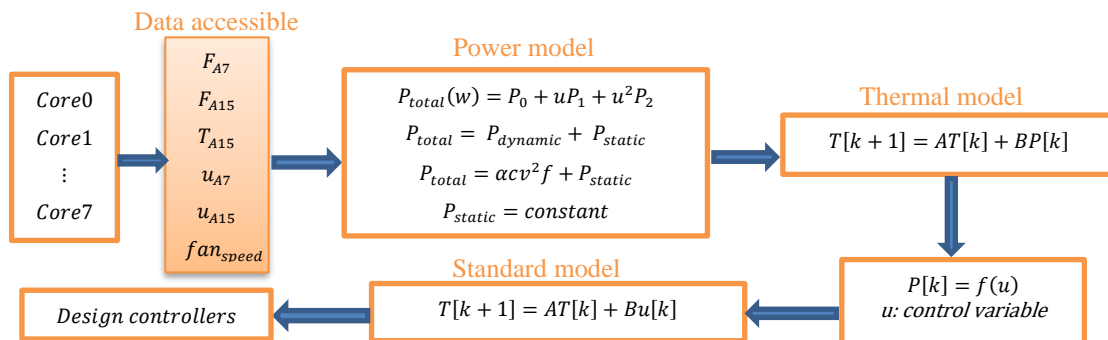


Figure 1. Proposed framework

### 3. MODEL GENERATION

Effective power and temperature management depends critically on accurate analytical models that can be evaluated at runtime. To achieve this goal, the model generation is divided into two parts: the power model and the thermal model. In the following, two models are described.

#### 3.1. Power model

Power consumption in the integrated circuits is the sum of two contributions: dynamic and static. The dynamic power can be expressed through (2) where  $\alpha$  and  $c$  are the activity factor and the switching capacitance [26]:

$$P_{total} = P_{dynamic} + P_{static} \quad (1)$$

$$P_{total} = \alpha c v^2_{dd} f + P_{static} \quad (2)$$

The total power is calculated indirectly using CPU utilization. CPU utilization is a simple tool for estimating the amount of computation that a CPU perform per time. According to Walker *et al.* [27] this method is used to calculate the total power for the ODROID-XU3 board. The ODROID-XU3 board has the same hardware specifications as ODROID-XU and the only difference between the two boards is that XU3 board has a voltage sensor. In this reference, the following is used to calculate power:

$$P_{total} = P_0 + uP_1 + u^2P_2 \quad (3)$$

where  $u$  represents CPU utilization and  $P_i$  coefficients for calculating total power are in accordance with the following table. Table 1 does not provide data for some operating frequencies such as 200 MHz and 1,700 MHz. For this purpose, using MATLAB curve fitting software, we obtain a relationship with a good accuracy for each coefficient. The accuracy of each relation and the of each coefficient are given in the Table 2.

Table 1. Values of  $P_i$  coefficients at different frequencies [27]

Freq (MHz)	$P_0$	$P_1$	$P_2$
250	0.010162804	0.001572937	-1.6E-06
300	0.009521533	0.001955864	-2.8E-06
350	0.010338362	0.002260855	-3.27E-06
400	0.012404617	0.002786165	-4.16E-06
450	0.014982476	0.003470516	-5.15E-06
500	0.019350116	0.004348964	-6.59E-06
550	0.023879147	0.005364183	-8.19E-06
600	0.029694786	0.006573153	-1.04E-05
800	0.036437558	0.015975673	-2.45E-05
900	0.043569437	0.018618245	-2.36E-05
1,000	0.05151296	0.022298895	-2.31E-05
1,100	0.06267777	0.026027083	-1.69E-05
1,200	0.071779829	0.029651724	-9.56E-06
1,300	0.082334714	0.03450953	8.47E-06
1,400	0.092116725	0.046563344	-9.22E-05
1,500	0.100661815	0.060414109	-0.000231806
1,600	0.113207437	0.071046296	-0.000356278

Table 2.  $P_i$  coefficient in terms of frequency

Coefficient	Equations	$R^2$
$P_0$	$2.939e - 8f^2 + 2.384e - 05f + 0.0001241$	0.9971
$P_1$	$(7.963e - 11)f^{2.786} + 0.002045$	0.9879
$P_2$	$-9.871e - 05 + 0.0001559 \cos(0.002327f) + 0.000173 \sin(0.002327f)$ $+ 0.0001407 \cos(0.002327f) - 0.0001495 \sin(0.002327f) - 6.48e$ $- 05 \cos(0.002327f) - 5.355e - 05 \sin(0.002327f)$	0.9803

$R^2$  is a measure of the goodness of model fitting

To obtain the values of the core voltages using the table given in [28] and using the MATLAB curve fitting toolbox, the voltage relation in terms of frequency is obtained as follows (The  $R^2$  fitness coefficients are above 0.99):

$$V_{a7} = 0.0000001963f_7^2 + 0.000004489f_7 + 0.8886 \quad (4)$$

$$V_{a15} = 0.0000001487f_{15}^2 - 0.0001167f_{15} + 0.9319 \quad (5)$$

### 3.2. Thermal model

The thermal model can presented as (6) [29]:

$$T[k + 1] = AT[k] + BP[k] \quad (6)$$

$T[k]$  and  $T[k + 1]$  are the observable temperature and the temperature in next time respectively. In order to obtain the coefficients of the, the power consumption and temperature are sampled in different workload. For this purpose, different benchmarks are used. The main use of these benchmarks is to affect the power consumption and performance of cores, including Mi-bench, Lm-bench, media-bench, and even scripts written by the user. For this purpose, 14 different tasks selected from the above sets have been used.

During the evaluation, we first set the temperature to 40 degrees and perform sampling. Also, to prevent damage to the board, we have selected the temperature threshold of 80 degrees. After passing this temperature, the fan performs cooling operation with maximum power.

It should be noted that for both clusters to be well included in the model, first we put one cluster at its minimum frequency and change the frequency of the other cluster by applying different workloads at an interval of 200 MHz from the lowest frequency to the highest frequency. In each frequency interval the temperature and estimated power are calculated. This is repeated for the other cluster and the sampling is done for 0%, 50%, and 100% of fan speed. After sampling the data, we obtain the unknown coefficients using the following relationships:

$$Y = X\Theta \quad (7)$$

where in:

$$X_{m \times 4} = [T[k] \ P_7[k] \ P_{15}[k] \ P_{fan}], \Theta_{4 \times 1} = [A \ B_7 \ B_{15} \ B_{fan}]^T, Y_{m \times 1} = T[k + 1] \quad (8)$$

$A$  is the current temperature coefficient,  $B_7$  is the little cluster power consumption coefficient,  $B_{15}$  is the big cluster power consumption coefficient,  $P$  is the power consumption of each element and  $m$  is the number of sampling data. Given that only the big cluster temperature is visible,  $T[k]$  is considered as the big cluster temperature and therefore no index is considered for it. To calculate the unknown coefficients, we use the recursive method:

$$(X^T X)\Theta = X^T Y \quad (9)$$

$$\Theta = (X^T X)^{-1} X Y \quad (10)$$

Given the sampling time  $\Delta t$ , the can be converted to a continuous [30]:

$$T[k + 1] = (1 + a\Delta t)T[k] + (B_7\Delta t)f_7[k] + (B_{15}\Delta t)f_{15}[k] + (B_{fan}\Delta t)u_{fan}[k] \quad (11)$$

$$\frac{T[k+1]-T[k]}{\Delta t} = aT[k] + B_7f_7[k] + B_{15}f_{15}[k] + B_{fan}u_{fan}[k] \quad (12)$$

$$T(t) = aT(t) + B_7f_7(t) + B_{15}f_{15}(t) + B_{fan}u_{fan}(t) \quad (13)$$

Finally, the continuous-time relationship can be express as (14):

$$\dot{T}(t) = 0.00176397T(t) + 0.07258447P_7 + 0.03656092P_{15} - 0.00095002u_{fan} \quad (14)$$

To access the standard form of describing state space, the  $P_7$  and  $P_{15}$  must be expressed in terms of frequency. Based on (2) and by simplifying, the final form of the is as (15):

$$T[k + 1] = AT[k] + (B_7 \ B_{15}) \begin{pmatrix} \alpha c_7 v_7^2 f_7 + P_{s7} \\ \alpha c_{15} v_{15}^2 f_{15} + P_{s15} \end{pmatrix} + B_{fan} u_{fan} \quad (15)$$

The linearization of the dynamic power terms in the P7 and P15 is done as shown in Table 3.

Table 3. Linear approximation of the product of dynamic power

Coefficient	$v_7^2 f_7$	$v_{15}^2 f_{15}$
The linear equation	$1.708f_7 - 385.2$	$1.648f_{15} - 499.9$
R <sup>2</sup>	0.9547	0.9372

The final relationship is obtained as (16):

$$\begin{aligned} \dot{T}(t) = & 0.00176397T(t) + [0.12397428\alpha_7f_7 + (-27.9595\alpha_7 + 0.0000047426)] \\ & + [0.06025242\alpha_{15}f_{15} + (-18.2768\alpha_{15} - 0.001934072)] \\ & - 0.00095002fan_{speed} \end{aligned} \quad (16)$$

### 3.3. Optimal controllers design

The purpose of designing optimal control is to achieve a control signal  $u(t)$  in the time interval  $t \in [t_0, t_f]$ . So that after applying the signal, the system observes desired performance by considering the physical constraints. To formulate optimal control problems, the following three principles must be examined: i) mathematical description of the system which is in the form of state-space; ii) expressing the physical limitations of the system; and iii) determining the performance index of the problem.

#### 3.3.1. State-space description

The description of the state space is in the form of (16). It can be rewritten as (17):

$$\dot{X}(t) = AX(t) + [B_7(t)u_7(t) + w_7(t)] + [B_{15}(t)u_{15}(t) + w_{15}(t)] + B_{fan}u_{fan}(t) \quad (17)$$

The coefficients  $w$  is obtained from the sum of the approximations of the of dynamic power with leakage power (the leakage power relationship is given in [31]) and can vary for each workload. The coefficients  $B_7(t)$  and  $B_{15}(t)$  are considered as variables due to the activity coefficient of each cluster.

#### 3.3.2. Physical constraints of the system

After obtaining the mathematical model, the physical constraints on the state variables and the control variables must be defined. These constraints are as:

$$200 \text{ MHz} \leq f_7 \leq 1400 \text{ MHz}$$

$$200 \text{ MHz} \leq f_{15} \leq 2000 \text{ MHz}$$

$$0 \leq u_{fan} \leq 255$$

On the ODROID\_XU4 board, the default control solution for fan speed control is shown in Table 4. The values [0 255] are for the 8-bit register of the PWM fan controller.

Table 4. Default fan speed control

Trip point	0	1	2
Temperature	45	50	55
Fan speed	150	190	252

#### 3.3.3. Performance index

To quantitatively evaluate the performance of the system, a performance index must be selected. The performance index is maximized or minimized in the optimal system. Given that our goal is to maintain system performance and temperature control, we select the performance index as (18):

$$J(u) = \int_{t_0}^{t_f} [\lambda + \gamma_7 u_7(t)^2 + \gamma_{15} u_{15}(t)^2 + \gamma_{fan} u_{fan}(t)^2] dt = \int_{t_0}^{t_f} g(t) dt \quad (18)$$

where  $J$  is the performance index,  $\lambda$  is the constant coefficient,  $\gamma$  is the coefficient for each control variable and  $u$  is the control variable. The coefficients of function are determined according to the required interval of the controllers to force the working load as (19):

$$J(u) = \int_{t_0}^{t_f} [0.5 + 0.000005f_{A7}(t)^2 + 0.0000025f_{A15}(t)^2 + 0.00025u_{fan}(t)^2] dt \quad (19)$$

In solving our problem, the above function must be minimized. In this case, this function is known as the cost function.

### 3.4. Optimal control theory

To solve the optimal control problem, we must control  $u^* \in u$  which causes the system:

$$\dot{x}(t) = Ax(t) + Bu(t) + w(t) = a(x(t), u(t), t) \quad (20)$$

*Temperature and performance evaluation of multiprocessors chips by optimal ... (Porya Soltani Hanafi Por)*

Finds an acceptable path and minimized the performance index. In terms of Hamilton, we have:

$$H(x(t), u(t), t) \triangleq g(x(t), u(t), t) + p^T(t)[a(x(t), u(t), t)] \quad (21)$$

P are known as Co-state. Necessary conditions for  $u^*$  is optimal control are:

$$\dot{x}^*(t) = \frac{\partial H}{\partial p}(x^*(t), u^*(t), p^*(t), t) \quad (22)$$

$$\dot{p}^*(t) = -\frac{\partial H}{\partial x}(x^*(t), u^*(t), p^*(t), t) \quad (23)$$

$$H(x^*(t), u^*(t), p^*(t), t) \leq H(x^*(t), u(t), p^*(t), t) \quad (24)$$

Lemma, if the:

$$\frac{\partial H}{\partial u}(x^*(t), (t), p^*(t), t) = 0 \quad (25)$$

Be established and the matrix:

$$\frac{\partial^2 H}{\partial u^2}(x^*(t), u^*(t), p^*(t), t) \quad (26)$$

Is also positive,  $u^*(t)$  is a sufficient condition for the controller design. Finally, using the mentioned relations, the control law for frequency controllers is obtained as (27):

$$u_i(t) = \begin{cases} \left( \frac{-(Ax+C) + \sqrt{(Ax+C)^2 + \frac{\lambda B^2}{\gamma}}}{B} \right) & ; x(t_1) < x(t) \leq x(t_2) \\ u_{min} & ; x(t_2) < x(t) \\ u_{max} & ; x(t) < x(t_1) \end{cases} \quad (27)$$

that:

$$x(t_1) = \frac{(\lambda - u_{max}^2 \gamma - u_{max} \frac{2\gamma C}{B})B}{u_{max}^2 \gamma A} \quad (28)$$

$$x(t_2) = \frac{(\lambda - u_{min}^2 \gamma - u_{min} \frac{2\gamma C}{B})B}{u_{min}^2 \gamma A} \quad (29)$$

and for fan speed controller:

$$u_i(t) = \begin{cases} +255 & ; x(t_1) < x(t) \\ \frac{(Ax) + \sqrt{(Ax)^2 + \frac{\lambda B^2}{\gamma}}}{B} & ; 0 < x(t) < x(t_1) \\ 0 & ; x(t) < 0 \end{cases} \quad (30)$$

that

$$x(t_1) = -\frac{(\lambda - 65025\gamma)B}{510\gamma A} \quad (31)$$

#### 4. EXPERIMENTAL EVALUATION

In this section, the performance of the proposed control method in the active and inactive states of the fan Odroid XU4 board and the execution time compared to the default state have been examined. The Odroid XU4 board uses the Samsung Exynos 5422 system-on-chip that integrates four Cortex-A15 (big) cores, and four Cortex-A7 (little) cores. The proposed methods are examined on common benchmarks, such as MP3, MP4 files, and Sysbench.

##### 4.1. Experiment 1

In this section, a motion picture experts group audio layer 3 (MP3) file of music with the executable time 3':45" is played and temperature variations are recorded for different  $\lambda$  as shown in Figure 2. Since this

test is a moderate workload for the processor, the fan is deactivated. As can be seen in Figures 3 and 4, as the  $\lambda$  coefficient in the performance index is increased, Clusters operate at higher frequencies, which increases the temperature. Also note that by increasing temperature, the purposed method decreases frequencies of the cores, which is the capability of the temperature reduction depends on the coefficient of the  $\lambda$ .

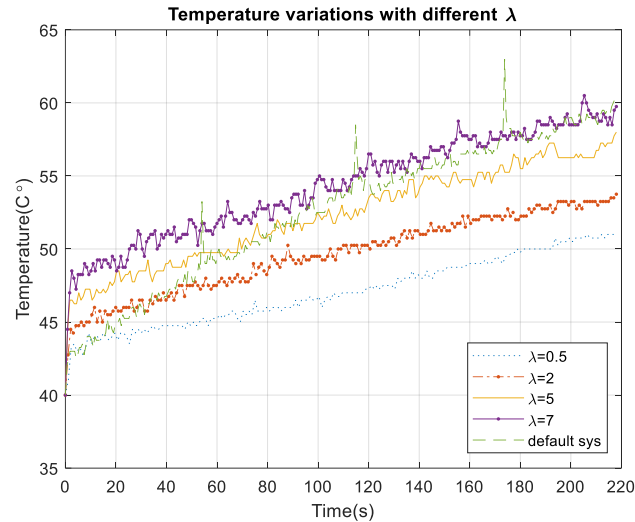


Figure 2. Temperature variations for different  $\lambda$

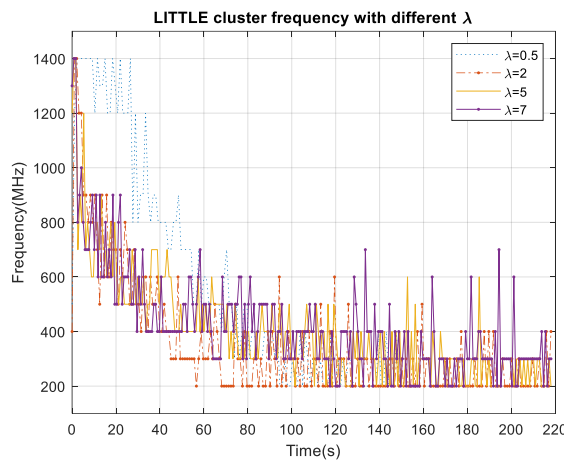


Figure 3. Behavior of A7 frequency for different  $\lambda$

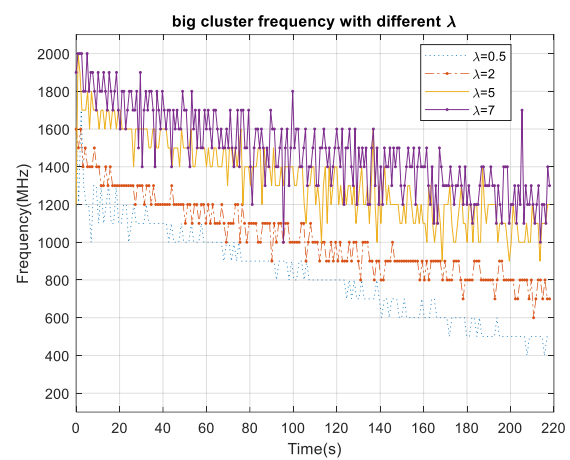


Figure 4. Behavior of A15 frequency for different  $\lambda$

#### 4.2. Experiment 2

In the second experiment, a MP4 file with the executable time 60 seconds is played. To evaluate the performance of control signals, this experiment is done in two states: without the fan and with the fan. In Figure 5 the fan is deactivated, the priority of purposed method is to reduce the temperature. It should be noted that since the workload and the controller are run simultaneously, the overhead causes the temperature to rise rapidly. But in the following, the slope of the temperature curve indicates that the proposed method reduces the temperature slope relative to the default state. Figure 6 and Figure 7 show the variation of A7 and A15 core frequency respectively in term of  $\lambda$  when the fan is not active.

The goal of the proposed method when the fan is activated is performance optimization with temperature constraints as shown in Figure 8. Also, it can be seen that the initial overhead in this curve is higher than the Figure 6. This overhead is expectable because the fan speed adjustment commands have been added to the previous control commands.

In Figure 8 although at  $\lambda=7$  the temperature is 3.5 degrees higher than the default, according to Figure 9, it is clear that the fan is working at 20% less speed. By changing the coefficient correctly, this

temperature difference can be compensated, but the fan speed power will be less than before. Increasing fan lifetime is one of the benefits of reducing fan speed, as developers and programmers make a trade-off between fan cooling power and temperature reduction. Figure 10 and Figure 11 show the variation of A7 and A15 core frequency respectively in term of  $\lambda$ .

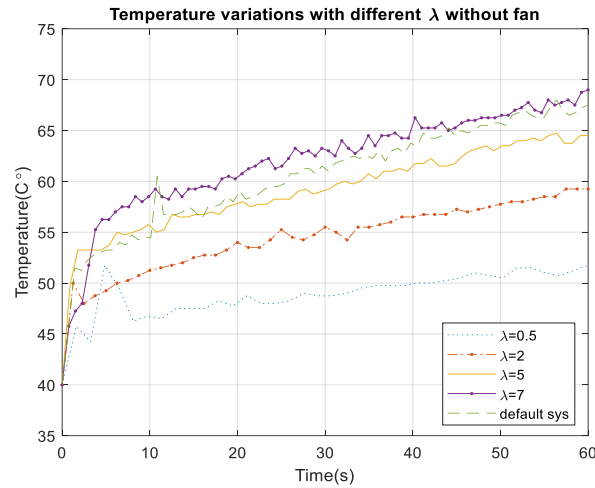


Figure 5. Temperature variations for different  $\lambda$

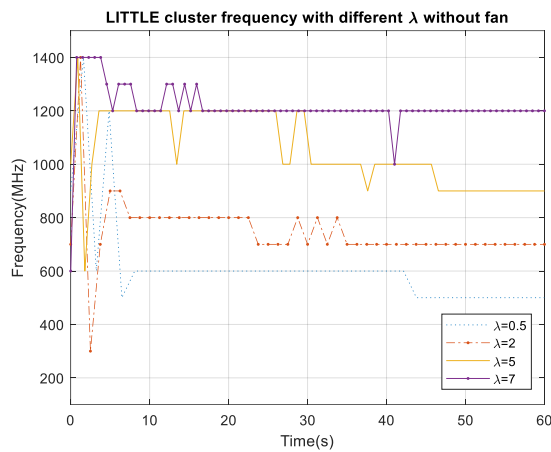


Figure 6. Behavior of A7 frequency for different  $\lambda$

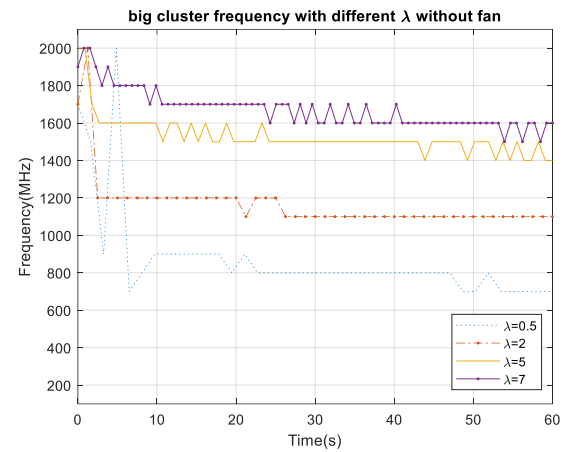


Figure 7. Behavior of A15 frequency for different  $\lambda$

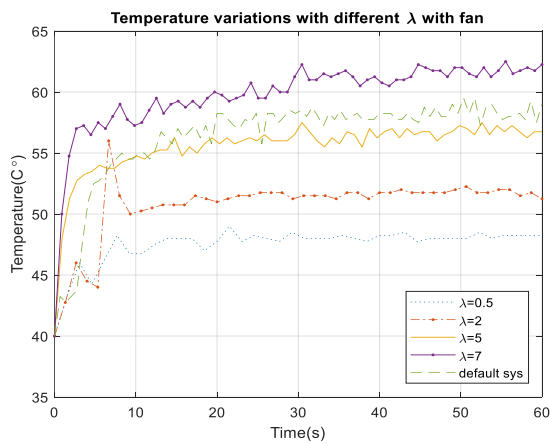


Figure 8. Temperature variations for different  $\lambda$

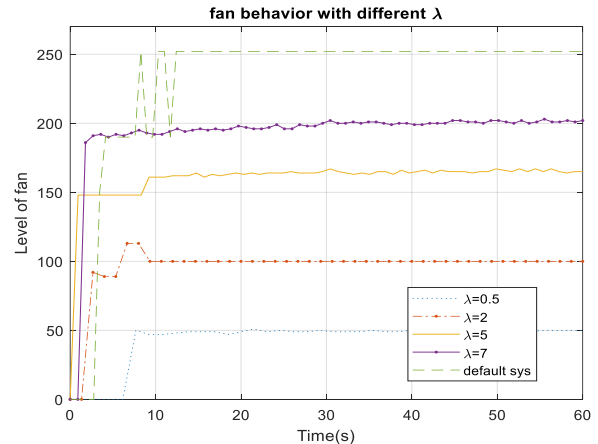
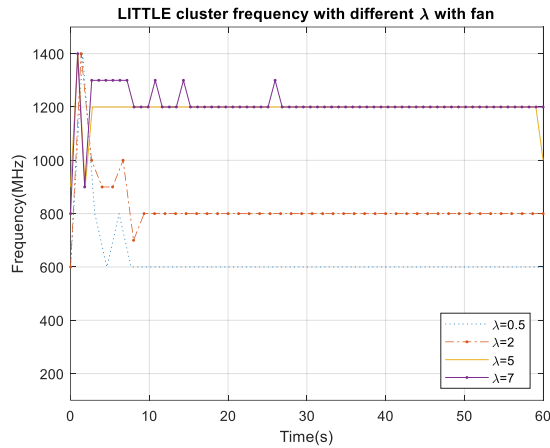
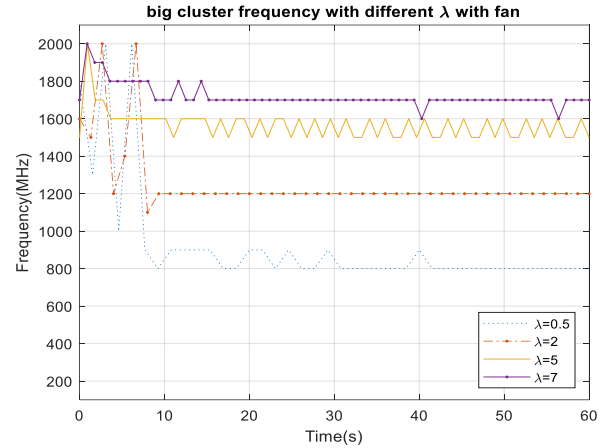


Figure 9. Behavior of fan speed for different  $\lambda$



Figure 10. Behavior of A7 frequency for different  $\lambda$ Figure 11. Behavior of A15 frequency for different  $\lambda$ 

It should be noted that the core frequency contains only the values 200, 300, ..., 2000 MHz. It is notable that the software of this board applies the frequency just in predefined values. For this reason, in the Figures 3, 4, 6, 7, 10, and 11 we observe just the predefined value of frequency. The commands for changing the frequency of core 1 in the Linux shell are shown in Figure 12. The frequency is in units of hertz (Hz).

```

root@odroid: /home/odroid/Desktop
File Edit View Search Terminal Help
root@odroid: /home/odroid/Desktop# cpufreq-set -c 1 -f 200000
root@odroid: /home/odroid/Desktop# cat /sys/devices/system/cpu/cpu0/cpufreq/cpuinfo_cur_freq
200000
root@odroid: /home/odroid/Desktop# cpufreq-set -c 1 -f 200001
root@odroid: /home/odroid/Desktop# cat /sys/devices/system/cpu/cpu0/cpufreq/cpuinfo_cur_freq
300000
root@odroid: /home/odroid/Desktop# cpufreq-set -c 1 -f 200000.84564
root@odroid: /home/odroid/Desktop# cat /sys/devices/system/cpu/cpu0/cpufreq/cpuinfo_cur_freq
300000
root@odroid: /home/odroid/Desktop#

```

Figure 12. Commands written in the Linux command line

### 4.3. Experiment 3

The efficiency of the proposed control in reducing the temperature was evaluated in two previous experiments. In this section, the performance of the board is measured by the runtime. The Sysbench benchmark was used to record the runtime. As the  $\lambda$  coefficient is increased, the runtime of the benchmark reduces. According to the Table 5, runtime for  $\lambda=0.5$  is degraded by 2x and for  $\lambda=12$  is upgrade by 1.0375x when compared to default controller.

Table 5. Impact of  $\lambda$  changes at runtime

$\lambda$	0.5	2	5	7	10	12	default
Runtime(s)	30.9399	22.9648	17.5474	16.2315	15.2118	14.9750	15.5376

Through the study in this paper, we can ensure that the control strategy can be expanded to trade-off between the energy savings and temperature control in multi processors systems. It should be noted that higher performance requires higher power consumption. As a result, higher performance can be interpreted as higher temperature and energy consumption.

## 5. CONCLUSION

With the ever increasing computational demand, the multi-processors systems undergo tremendous thermal stress that has a detrimental effect on the system reliability. Many of the proposed DTM techniques do not consider the frequency and the fan speed as control variables simultaneously and were limited to one. Consequently, these techniques can be considered incomplete. In this paper, we solve the above problem with the optimal control methods. Also, by obtaining an accurate thermal model, control goals, including temperature and performance control are examined by changing the  $\lambda$  coefficient in the cost function. The choice of this coefficient is very important in the behavior of controllers. The experiments were performed to demonstrate the effectiveness of the proposed method for various purposes as well. In the first and second experiments, it is shown that the algorithm proposed can reduce the temperature and also the fan speed power by about 20%. In the final experiment, the results manifest the effectiveness of the proposed method in the performance. In the future research work, we want to use a multiprocessor system with temperatures sensors for all of cores that examine the interaction effect and improve the efficiency of the proposed control method.




## REFERENCES

- [1] Q. Bashir, M. N. Shehzad, M. N. Awais, S. Baig, M. G. Dogar, and A. Rashid, "An online temperature-aware scheduling technique to avoid thermal emergencies in multiprocessor systems," *Computers and Electrical Engineering*, vol. 70, pp. 83–98, 2018, doi: 10.1016/j.compeleceng.2018.06.002.
- [2] K. M. Attia, M. A. El-Hosseini, and H. A. Ali, "Dynamic power management techniques in multi-core architectures: A survey study," *Ain Shams Engineering Journal*, vol. 8, no. 3, pp. 445–456, Sep. 2017, doi: 10.1016/j.asej.2015.08.010.
- [3] M. Frankiewicz and A. Kos, "Microprocessor frequency control method under thermal and energy savings constraints," *IEEE Transactions on Components, Packaging and Manufacturing Technology*, vol. 5, no. 12, pp. 1755–1762, Dec. 2015, doi: 10.1109/TCPMT.2015.2496876.
- [4] J. Park and H. Cha, "Aggressive voltage and temperature control for power saving in mobile application processors," *IEEE Transactions on Mobile Computing*, vol. 17, no. 6, pp. 1233–1246, Jun. 2018, doi: 10.1109/TMC.2017.2762670.
- [5] R. Salvador, A. Sanchez, X. Fan, and T. Gemmeke, "A cortex-M3 based MCU featuring AVS with 34nW static power, 15.3 pJ/inst. active energy, and 16% power variation across process and temperature," in *ESSCIRC 2018-IEEE 44th European Solid State Circuits Conference*, 2018, pp. 206–209, doi: 10.1109/ESSCIRC.2018.8494312.
- [6] J. Donald and M. Martonosi, "Techniques for multicore thermal management: Classification and new exploration," in *33rd International Symposium on Computer Architecture (ISCA '06)*, 2006, pp. 78–88, doi: 10.1109/ISCA.2006.39.
- [7] O. Sahin, P. T. Varghese, and A. K. Coskun, "Just enough is more: Achieving sustainable performance in mobile devices under thermal limitations," in *2015 IEEE/ACM International Conference on Computer-Aided Design (ICCAD)*, Nov. 2015, pp. 839–846, doi: 10.1109/ICCAD.2015.7372658.
- [8] A. M. C. Demetrios *et al.*, "Performance and energy trade-offs for parallel applications on heterogeneous multi-processing systems," *Energies*, vol. 13, no. 9, pp. 1–24, May 2020, doi: 10.3390/en13092409.
- [9] S. K. Sahoo, M. K. Das, and P. Rath, "Application of TCE-PCM based heat sinks for cooling of electronic components: A review," *Renewable and Sustainable Energy Reviews*, vol. 59, pp. 550–582, Jun. 2016, doi: 10.1016/j.rser.2015.12.238.
- [10] J. Choi, M. Jeong, J. Yoo, and M. Seo, "A new CPU cooler design based on an active cooling heatsink combined with heat pipes," *Applied Thermal Engineering*, vol. 44, pp. 50–56, Nov. 2012, doi: 10.1016/j.applthermaleng.2012.03.027.
- [11] A. Siricharoenpanich, S. Wiriyaart, A. Srichat, and P. Naphon, "Thermal management system of CPU cooling with a novel short heat pipe cooling system," *Case Studies in Thermal Engineering*, vol. 15, pp. 1–8, Nov. 2019, doi: 10.1016/j.csite.2019.100545.
- [12] T. Yousefi, S. A. Mousavi, B. Farahbakhsh, and M. Z. Saghir, "Experimental investigation on the performance of CPU coolers: Effect of heat pipe inclination angle and the use of nanofluids," *Microelectronics Reliability*, vol. 53, no. 12, pp. 1954–1961, Dec. 2013, doi: 10.1016/j.microrel.2013.06.012.
- [13] M. Nazari, M. Karami, and M. Ashouri, "Comparing the thermal performance of water, Ethylene Glycol, Alumina and CNT nanofluids in CPU cooling: Experimental study," *Experimental Thermal and Fluid Science*, vol. 57, pp. 371–377, Sep. 2014, doi: 10.1016/j.expthermflusci.2014.06.003.
- [14] K. Skadron, T. Abdelzaher, and M. R. Stan, "Control-theoretic techniques and thermal-RC modeling for accurate and localized dynamic thermal management," in *Proceedings Eighth International Symposium on High Performance Computer Architecture*, 2002, pp. 17–28, doi: 10.1109/HPCA.2002.995695.
- [15] D. Huang, A. Pahlevan, M. Zapater, and D. Atienza, "COCKTAIL: Multi-core co-optimization framework with proactive reliability management," *IEEE Transactions on Computer-Aided Design of Integrated Circuits and Systems*, vol. 41, no. 2, pp. 386–399, Feb. 2022, doi: 10.1109/TCAD.2021.3058959.
- [16] M. Mohaqeqi, M. Kargahi, and K. Fouladi, "Stochastic thermal control of a multicore real-time system," in *2016 24th Euromicro International Conference on Parallel, Distributed, and Network-Based Processing (PDP)*, Feb. 2016, pp. 208–215, doi: 10.1109/PDP.2016.44.
- [17] H. R. Pourshaghghi, H. Fatemi, and J. P. de Gyvez, "Sliding-mode control to compensate PVT variations in dual core systems," in *2012 Design, Automation & Test in Europe Conference & Exhibition (DATE)*, Mar. 2012, pp. 1048–1053, doi: 10.1109/DATE.2012.6176650.
- [18] Y. Cui, W. Zhang, and B. He, "A variation-aware adaptive fuzzy control system for thermal management of microprocessors," *IEEE Transactions on Very Large Scale Integration (VLSI) Systems*, vol. 25, no. 2, pp. 683–695, Feb. 2017, doi: 10.1109/TVLSI.2016.2596338.
- [19] H. Chen, Y. Han, G. Tang, and X. Zhang, "Modeling and deep explicit model predictive control for server processor direct liquid cooling," in *2019 IEEE 21st Electronics Packaging Technology Conference (EPTC)*, Dec. 2019, pp. 154–157, doi: 10.1109/EPTC47984.2019.9026588.
- [20] J. M. N. Abad and A. Soleimani, "A neuro-fuzzy fan speed controller for dynamic management of processor fan power consumption," in *2016 1st Conference on Swarm Intelligence and Evolutionary Computation (CSIEC)*, Mar. 2016, pp. 148–153, doi: 10.1109/CSIEC.2016.7482121.
- [21] Q. Fang, J. Wang, Q. Gong, and M. Song, "Thermal-aware energy management of an HPC data center via two-time-scale




- control,” *IEEE Transactions on Industrial Informatics*, vol. 13, no. 5, pp. 2260–2269, Oct. 2017, doi: 10.1109/TII.2017.2698603.
- [22] R. Ayoub, K. Indukuri, and T. S. Rosing, “Temperature aware dynamic workload scheduling in multisocket CPU servers,” *IEEE Transactions on Computer-Aided Design of Integrated Circuits and Systems*, vol. 30, no. 9, pp. 1359–1372, Sep. 2011, doi: 10.1109/TCAD.2011.2153852.
- [23] M. A. Elsayaf, H. A. Fahmy, and A. L. Elshafei, “CPU dynamic thermal management via thermal spare cores,” in *2009 25th Annual IEEE Semiconductor Thermal Measurement and Management Symposium*, 2009, pp. 139–145, doi: 10.1109/STHERM.2009.4810755.
- [24] Y. Fu, N. Kottenstette, C. Lu, and X. D. Koutsoukos, “Feedback thermal control of real-time systems on multicore processors,” in *Proceedings of the tenth ACM international conference on Embedded software - EMSOFT '12*, 2012, pp. 113–122, doi: 10.1145/2380356.2380379.
- [25] N. Ahmed, A. L. C. Barczak, M. A. Rashid, and T. Susnjak, “Runtime prediction of big data jobs: Performance comparison of machine learning algorithms and analytical models,” *Journal of Big Data*, vol. 9, no. 1, pp. 1–31, Dec. 2022, doi: 10.1186/s40537-022-00623-1.
- [26] G. Singla, G. Kaur, A. K. Unver, and U. Y. Ogras, “Predictive dynamic thermal and power management for heterogeneous mobile platforms,” in *Design, Automation & Test in Europe Conference & Exhibition (DATE)*, 2015, pp. 960–965, doi: 10.7873/DATE.2015.1036.
- [27] M. J. Walker, A. Das, G. Merrett, and B. M. Hashimi, “Run-time power estimation for mobile and embedded asymmetric multi-core CPUs,” 2015.
- [28] R. Gensh *et al.*, “Experiments with Odroid-XU3 Board,” 2015.
- [29] S. Reda and A. Belouchrani, “Blind identification of power sources in processors,” in *Design, Automation & Test in Europe Conference & Exhibition (DATE)*, 2017, Mar. 2017, pp. 1739–1744, doi: 10.23919/DATE.2017.7927274.
- [30] D. E. Kirk, *Optimal control theory: An introduction*. Chelmsford: Courier Corporation, 2004.
- [31] I. H. Baek and X. Liu, “Power and energy analysis on Odroid-XU+ E and adaptive power model,” 2017.

## BIOGRAPHIES OF AUTHORS






**Porya Soltani Hanafi Por**    received the B.S. degree in electrical and electronics engineering from Bu-Ali Sina University, Hamedan, Iran, in 2017, and the M.S. degree in control engineering from Bu-Ali Sina University, Hamedan, Iran, in 2021. He spent her internship in Shahid Mofteh power plant, in Hamedan, in 2017. His research interests include energy-performance optimization in computing systems, dynamic thermal and power management for multicore chips. He can be contacted at email: porya.soltani.hanafi.por@gmail.com.



**Abbas Ramazani**    received the B.S. degree in electronics engineering from the Isfahan University of Technology, Isfahan, Iran, in 1991, the M.S. degree from Tarbiat Modarres University, in telecommunications engineering, in 1995, Tehran, Iran and Ph.D. degree in microelectronics from the University of Lorraine, Metz, France, in 2005. He was with Iranian Research Centre of Telecommunication from 1993 to 1995. He was with Lorestan University as instructor from 1995 to 2000 and as Assistant Professor from 2005 to 2015. He is currently an Assistant Professor of Electrical Engineering at Bu Ali Sina University, Hamedan, Iran. He has published numerous papers in his field of research, which includes the microprocessors architecture, fault tolerant architecture, VLSI design, low power design, and digital signal processing. He can be contacted at email: a.ramazani@basu.ac.ir.



**Mojtaba Hosseini Toodeshki**    received the B.S., M.S., and Ph.D degrees in control branch of electrical engineering from Isfahan University of Technology (IUT), Isfahan, Iran, in 2000, 2003 and 2010 respectively. He is currently an assistant professor in the group of electrical engineering, branch of control, at the Hamedan University of Technology (HUT), Iran. His current research interests include robust control, adaptive control, and optimal control for nonlinear and time delay systems. He can be contacted at email: mhosseini.t@hut.ac.ir.